Simplest piston problem. II. Inelastic collisions

Pablo I. Hurtado[1,2,*] and S. Redner[3,†]
[1]*Institute Carlos I for Theoretical and Computational Physics, Universidad de Granada, 18071 Granada, Spain*
[2]*Department of Physics, Boston University, Boston, Massachusetts 02215, USA*
[3]*Theoretical Division and Center for Nonlinear Studies, Los Alamos National Laboratory, Los Alamos, New Mexico 87545, USA*
(Received 28 July 2005; published 27 January 2006)

We study the dynamics of three particles in a finite interval, in which two light particles are separated by a heavy "piston," with elastic collisions between particles but inelastic collisions between the light particles and the interval ends. A symmetry breaking occurs in which the piston migrates near one end of the interval and performs small-amplitude periodic oscillations on a logarithmic time scale. The properties of this dissipative limit cycle can be understood simply in terms of a effective restitution coefficient picture. Many dynamical features of the three-particle system closely resemble those of the many-body inelastic piston problem.

DOI: 10.1103/PhysRevE.73.016137 PACS number(s): 02.50.Ey, 05.20.Dd, 45.05.+x, 45.50.Tn

I. INTRODUCTION

In the preceding paper, denoted as HR [1], we discussed the collision dynamics of an elastic three-particle system on a finite interval that consists of a massive particle—a piston—that separates two lighter particles. The motivation for studying this idealized system was to shed light on the enigmatic piston problem [2], where a gas-filled container is divided into two compartments by a heavy but freely moving piston. When the gases in each compartment have different initial thermodynamic states and when the piston moves without friction, the approach to equilibrium is unexpectedly complex and still incompletely understood [3–6].

As discussed in HR, some of the rich phenomenology of the piston problem can be captured by the much simpler three-particle system in a finite interval. To understand the evolution of the latter system, it proved convenient to map the trajectories of the three particles on the line onto an equivalent elastic billiard particle that moves within a highly skewed tetrahedral region, with the specular reflection whenever the billiard hits the tetrahedron boundaries [7–11]. From this simple geometrical mapping, we deduced several anomalous dynamical properties of the three-particle system, such as the power-law distribution of time intervals for the piston to make successive crossings of the interval midpoint.

In the inelastic piston problem, the collisions between the constituent particles in the gas are inelastic, so that each gas undergoes inelastic collapse if either the number of particles is sufficiently large or the restitution coefficient is sufficiently small. Recent work by Brito *et al.* [12] has again discovered surprisingly rich dynamics, very different in character from the elastic case, in which one of the gases cools more quickly and gets compressed into a solid by the piston. An even stranger feature is that this compression is not monotonic, but rather the piston has superimposed oscillations whose period grows exponentially with time. Thus the cooling of the inelastic piston problem is much richer than that of the classical inelastic gas problem [13].

Given the complex behavior exhibited by the many-body piston system, we are again led to investigate a simpler alternative: a three-particle system in the unit interval that contains a heavy piston that lies between two light particles. Collisions between light particles and the ends of the interval (henceforth termed walls) are inelastic, to mimic the many-particle piston problem when the gases are inelastic, while the collisions between the particles and the piston are elastic.

When the light particles have the same initial energy but nonsymmetric positions, one light particle loses energy more quickly than the other. As a consequence, the piston migrates to the wall that is closer to the cooler light particle. Somewhat unexpectedly, a typical system eventually falls into a periodic state on a logarithmic time scale where the piston undergoes small-amplitude oscillations near one wall with a constant period in $\ln t$, while the light particles undergo complementary oscillatory motions. We term this phenomenon as the log-periodic state. Another intriguing aspect of the three-particle system is that it closely mirrors the time evolution in the many-particle inelastic piston system [12]. Thus we are able to understand features of the many-body problem in terms of simple physical pictures that arise from studying the three-particle system on the interval.

In the next section, we describe the two basic dynamical features of the three-particle system, namely, the initial symmetry breaking and the log-periodic state. We then give a macroscopic description of the collapse process and the subsequent oscillatory motion of the piston in Sec. III. Finally, in Sec. IV, we develop an effective restitution coefficient description for the particle collisions that accounts for many of our observations. Various calculational details are given in an appendix.

II. BASIC PHENOMENOLOGY

A. Symmetry breaking

For the many-body system in which the gases on either side of the piston are inelastic and have identical macroscopic initial conditions, Brito *et al.* [12] found an instability

*Email address: phurtado@onsager.ugr.es
†Permanent address: Department of Physics, Boston University, Boston, Massachusetts 02215, USA. Email address: redner@bu.edu

 ©2006 The American Physical Society

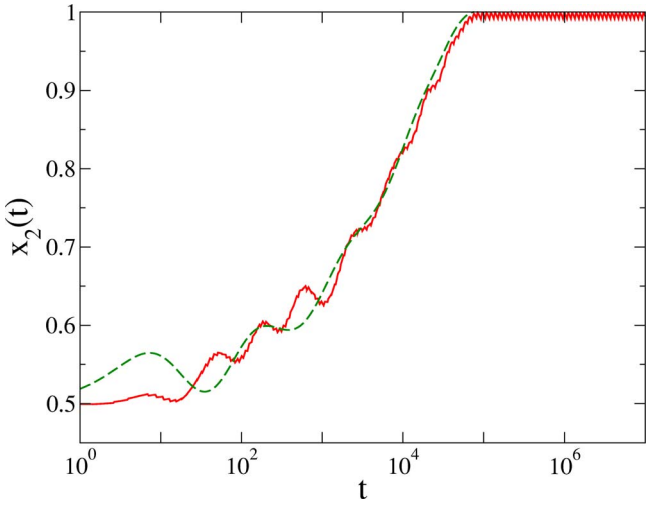

FIG. 1. (Color online) Piston position $x_2(t)$ versus t on a logarithmic time scale for $m_2=100$ and $r=0.9$. The solid curve is the simulation result while the dashed curve is the prediction from the macroscopic equations of motion, Eqs. (3)–(5).

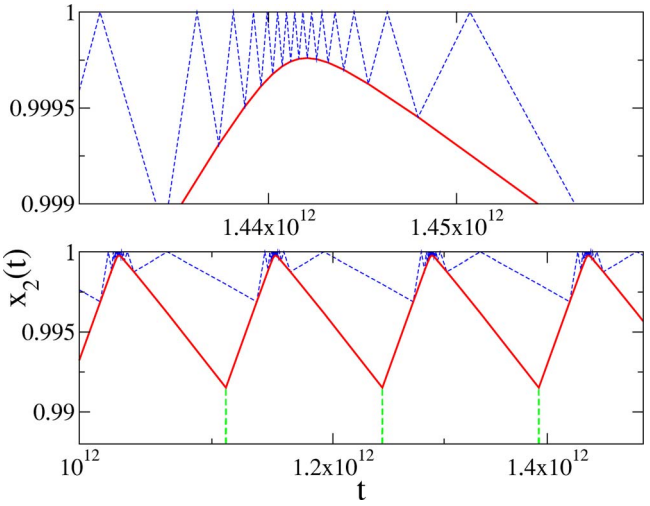

FIG. 2. (Color online) Magnification of the long-time evolution in Fig. 1. Bottom: The log-periodic state. Top: Detail of a "rattling" collision sequence between the piston and the trapped light particle.

in which one of the gases cools more rapidly and the piston ultimately compresses the cooler gas into a solid. While such an instability seems intuitively plausible, an unexpected feature is that the piston moves nonmonotonically during this cooling, with regular oscillations that are periodic on a logarithmic time scale. In this section, we show that much of this phenomenology also arises in the idealized three-particle system on the unit interval.

The particles are located at x_1, x_2, and x_3, with $0 \leqslant x_1 \leqslant x_2 \leqslant x_3 \leqslant 1$. The light particles, with masses $m_1=m_3=1$ and locations x_1 and x_3, collide elastically with a massive piston with mass $m_2 \gg 1$ at x_2 and inelastically with the walls. Thus a light particle that hits a wall with speed $v=\sqrt{2E}$ is reflected with speed rv, where $r \in [0,1]$ is the restitution coefficient. The energy change in this collision is $\Delta E=-E(1-r^2)<0$.

Figure 1 shows a representative result for the piston position $x_2(t)$ versus t on a logarithmic scale for the case $m_2=100$ and $r=0.9$. The initial velocities are $(v_1(0),v_2(0),v_3(0))=(1,0,-1)$ so that two light particles approach the piston with equal and opposite velocities. Thus the system initially has zero momentum and total energy $E=1$. The initial positions of the light particles were chosen uniformly in $(0,1/2)$ and in $(1/2,1)$; for the example of Fig. 1, $(x_1(0),x_2(0),x_3(0))=(0.083\,25,0.5,0.862\,83)$. As a result, the first collision is between the piston and particle 3. This small initial asymmetry eventually drives the piston from oscillations about $x_2=1/2$ to the nonsymmetric long-time behavior depicted in Fig. 1. It bears emphasizing that the phenomenology of the three-particle system up to approximately 10^5 time steps is qualitatively similar to that of the many-particle inelastic piston problem [12].

In the long-time limit, the piston migrates close to one of the walls. Which of the two walls is selected is determined by the identity of the first collision. When the piston is initially located at $x_2=1/2$ and the two particles approach with equal and opposite velocities, the piston is driven to the right wall if the first collision occurs with its right neighbor and *vice versa*. The light particle that first hits the piston then collides earliest with the wall and begins cooling earlier. This fact leads to the piston eventually compressing the particle that experiences the first collision with a wall.

B. The log-periodic state

Numerically, we find that the three-particle system asymptotically falls into a log-periodic state—where the piston undergoes small-amplitude oscillations with a constant period in $\ln t$—for almost all initial conditions. In this state, one of the light particles is trapped in a small gap between the piston and the wall (Fig. 2), while the other light particle has most of the energy and travels over almost the entire interval.

During these oscillations, the light particle that is compressed by the piston performs a sequence of violent rattlings each time the piston approaches and eventually is reflected by the nearer wall (top panel in Fig. 2). The piston then collides with the other light particle whose energy is nearly equal to that of the entire system and whose momentum is comparable in magnitude to that of the piston. After this collision, the piston is reflected back toward the nearer wall and the rattling sequence with the trapped light particle begins anew.

Generally this long-time state has a one-cycle periodicity in which the position of the piston recurs at each maximum of its oscillation cycle (Fig. 2). However, for piston mass m_2 less that a r-dependent threshold mass $\mu_t(r)$, we empirically find that the asymptotic state can be a two-cycle, three-cycle, etc., with lower cycles more likely to occur than high cycles. Conversely, for m_2 greater than an upper threshold

$$\mu_c(r) = \frac{(1+r)(1+r+4\sqrt{r})+4r}{(1-r)^2}, \tag{1}$$

inelastic collapse occurs, where the piston ultimately sticks to a wall (see the Appendix for the derivation of μ_c). For the purposes of the present discussion, we are interested in the

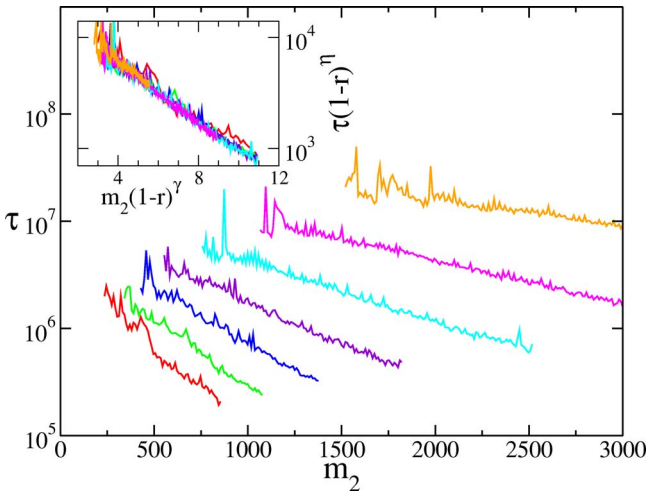

FIG. 3. (Color online) Plot of τ as a function of m_2 on a semilogarithmic scale, for restitution coefficients r=0.875, 0.8875, 0.9, 0.9125, 0.925, 0.9375, and 0.95 (bottom to top). The inset shows the data collapse of τ for different values of r using γ=2.1 and η=2.6.

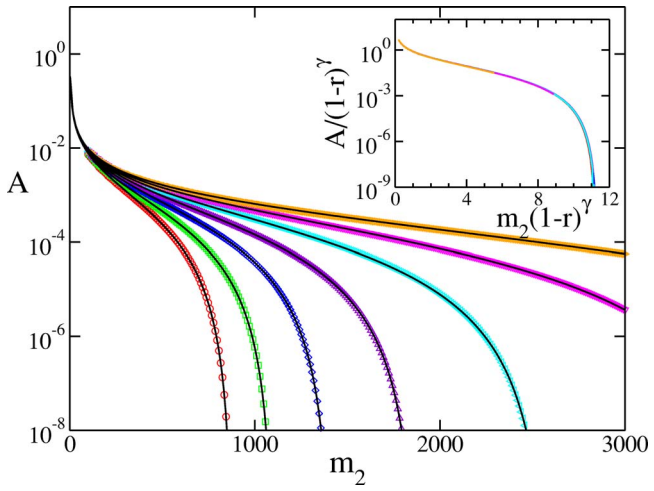

FIG. 4. (Color online) The amplitude of the log-periodic oscillations, A, as a function of the piston mass on a semilogarithmic scale for the same r values as in Fig. 3 (data shifting to the right for increasing r). The curves are the predictions from Eq. (12), based on an effective restitution coefficient picture (see text). Inset: Data collapse of A for different values of r and γ=2.1.

case where m_2 is in the range $[\mu_t(r),\mu_c(r)]$ so that the system falls into a one-cycle log-periodic state.

This state may be characterized by the relaxation time $\tau(m_2,r)$ until the piston settles into the log-periodic motion and the amplitude, $A(m_2,r)$, and period on a logarithmic time scale, $\Delta(m_2,r)$, of the ensuing oscillations. The latter is defined via $t_{k+1}=e^{\Delta}t_k$, where t_k and t_{k+1} are the times for two consecutive maxima of $x_2(t)$ in the final state (bottom panel in Fig. 2).

Figure 3 shows the relaxation time τ as a function of m_2 for m_2 in the range $[\mu_t,\mu_c]$ for representative values of r. We expect that the oscillatory regime is reached more quickly for larger m_2 since energy is more quickly dissipated when the piston is heavier, as confirmed by the data. We also find that τ decays exponentially with m_2, that is, $\tau\sim\exp[-m_2/\mu(r)]$, with a characteristic mass scale $\mu(r)$ that is nearly equal to the threshold mass $\mu_t(r)$. Both μ and μ_t numerically scale as $(1-r)^{-\gamma}$ for r close to 1, with $\gamma\approx 2.1$. This is slightly larger than the anticipated exponent value of 2 that is based on the hypothesis that there should be only one characteristic mass that scales as $\mu_c\sim(1-r)^{-2}$ in the limit $r\to 1$ from Eq. (1). We attribute the discrepancy in γ to corrections to scaling; the largest restitution coefficient r=0.95 that is practical to study is still not very close to 1.

When the piston is in the log-periodic state, the amplitude A is a monotonically decreasing function of m_2 and vanishes as $m_2\to\mu_c(r)$, signaling the onset of inelastic collapse (Fig. 4). The logarithmic period of the oscillations Δ (not shown) scales approximately as $\Delta(m_2,r)\approx(1-r)$ and depends weakly on m_2.

Because these three characteristics of the oscillations—τ, A, and Δ—seem to be governed by the same mass scale, we anticipate that data collapse will occur. Empirically, we find that these quantities are consistent with the scaling forms

$$\tau(m_2,r)\sim(1-r)^{-\eta}\Phi_\tau[m_2(1-r)^\gamma],$$

$$A(m_2,r)\sim(1-r)^{\gamma}\Phi_A[m_2(1-r)^\gamma],$$

$$\Delta(m_2,r)\sim(1-r)\Phi_\Delta[m_2(1-r)^\gamma], \quad (2)$$

with $\gamma\approx 2.1$. Additionally, $\eta\approx 2.6$ is an apparently independent exponent that characterizes the relaxation time τ, while Φ_τ, Φ_A, and Φ_Δ are scaling functions. The insets to Figs. 3 and 4 show that the data collapse for τ and A is quite good.

Although the asymptotic state of the system is periodic on a logarithmic time scale, we emphasize that the total energy of the system, $E(t)$, continues to dissipate due to inelastic collisions with the walls. At a coarse-grained level, we recover Haff's law [14] $E(t)\sim t^{-2}$ (upper curve in Fig. 5), as expected. Notice that for the specific example being studied (in which the piston compresses particle 3), $E(t)\approx E_1(t)$. At a

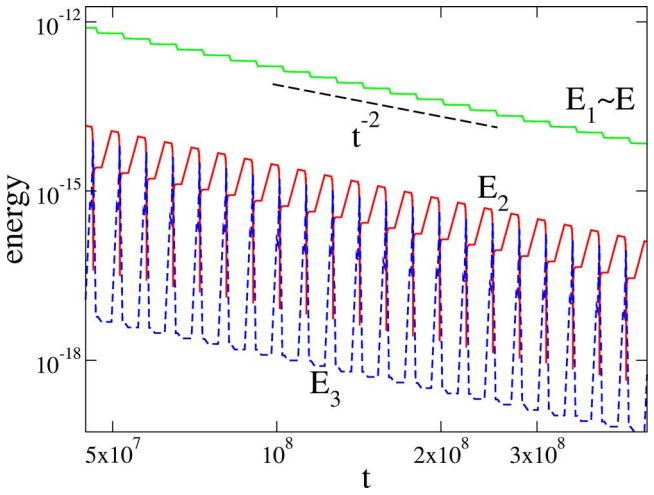

FIG. 5. (Color online) Energy of each particle as a function of time on a double logarithmic scale for the system depicted in Fig. 1.

finer time scale, however, $E(t)$ undergoes a sequence of steps and almost constant plateaus. The largest drop in energy occurs when the more energetic light particle collides with the wall, while the rattling dynamics between the piston and the other light particle leads to a small decrease in the energy of the system.

III. MACROSCOPIC DESCRIPTION

We can understand the initial instability of the piston in terms of macroscopic equations of motion [12,14]. The macroscopic approach given here ostensibly applies for any value of the restitution coefficient r for fixed piston mass m_2, or equivalently for any m_2 for fixed r. In particular, this approach correctly describes the initial instability of the inelastic piston for any value of the parameters r and m_2. The only feature that the macroscopic approach fails to describe is the final state for piston masses below the critical mass, $m_2 < \mu_c$.

According to the macroscopic description, the energies of the light particles change in time by two processes. First, the energy decreases due to inelastic collisions with the walls. This cooling is macroscopically described by Haff's law, in which the energy change is proportional to the particle energy and the number of collisions per unit time. Thus $dE_i(t)|_{\rm coll} = -E_i(t)(1-r^2)n_{\rm coll}(t)dt$, with $i=1,3$. The collision rate may be approximated by $n_{\rm coll}(t) \approx \sqrt{2E_i(t)}/\ell_i(t)$, where $\sqrt{2E_i(t)}$ is the thermal velocity and $\ell_i(t)$ is the length of the region available for particle i; thus $\ell_1(t) = x_2(t)$ and $\ell_3(t) = 1 - x_2(t)$. On the other hand, the energies of the light particles also change because of compression or expansion by the piston. The macroscopic equation describing this process is $dE_i(t)|_{\rm piston} = -P_i d\ell_i$, $i=1,3$, where P_i is the pressure exerted on particle i, and $d\ell_i$ is the length change

Assuming the ideal gas law $P_i = T_i/\ell_i$ (Boltzmann's constant is set to 1), and writing $T_i = 2E_i$, we obtain

$$\frac{dE_1}{dt} = -2E_1\frac{v_2}{x_2} - \sqrt{2}(1-r^2)\frac{E_1^{3/2}}{x_2}, \tag{3}$$

$$\frac{dE_3}{dt} = 2E_3\frac{v_2}{1-x_2} - \sqrt{2}(1-r^2)\frac{E_3^{3/2}}{1-x_2}. \tag{4}$$

This is essentially the approach of Haff [14] for the inelastic gas, and it was also adopted for the inelastic many-particle piston problem of Brito *et al.* [12]. The force exerted on the piston is given by the pressure difference, $P_1 - P_2$, so that the macroscopic equation of motion for the piston is

$$m_2\frac{{\rm d}^2x_2}{{\rm d}t^2} = \frac{2E_1}{x_2} - \frac{2E_3}{1-x_2}. \tag{5}$$

Equations (3)–(5) describe the evolution of the three-particle system on a coarse-grained time scale and they are the analogs of the equations derived in Ref. [12] for the many-body inelastic piston problem.

A particular solution to these macroscopic equations is symmetric cooling of both light particles, $E_1(t) = E_3(t) = E_0[1+\sqrt{2E_0}(1-r^2)t]^{-2}$, with E_0 the initial light particle energy, while the piston remains at $x_2(t) = 1/2$. However, linear perturbation analysis shows that any small disturbance from symmetry grows and the piston is driven toward one of the walls, with an oscillatory modulation that is periodic on logarithmic time scale [12].

A typical piston trajectory that is obtained by numerically solving Eqs. (3)–(5) with a slightly asymmetrical state is shown in Fig. 1. The numerical solution to the macroscopic equations and the simulation results for the three-particle system are extremely close over the time range $10^3 < t < 10^5$. However, after approximately 10^5 time steps (for the case $m_2 = 100$ and $r = 0.9$), the macroscopic equations predict that inelastic collapse occurs, after which the piston sticks to one of the walls [12]. In contrast, for the three-particle system, the piston localizes near one wall but continues to undergo small-amplitude, nearly regular oscillations on a logarithmic time scale (Fig. 2).

To help understand this discrepancy between the macroscopic approach and the simulations results for the three-particle system in the long-time limit, it is helpful to reconsider the elastic case $r=1$. Here Eqs. (3) and (4) can be immediately integrated, and substituting the results of these integrations into (5) gives

$$m_2\frac{{\rm d}^2x_2}{{\rm d}t^2} = \frac{A_1}{x_2^3} - \frac{A_3}{(1-x_2)^3},$$

where $A_{1,3}$ are constants. This equation of motion describes the oscillations of a particle in the effective potential well $V_{\rm eff}(x) = \frac{1}{2}[A_1x^{-2} + A_3(1-x)^{-2}]$. This effective potential can be derived rigorously in the limit $m_2 \to \infty$ (see [15] and also the Appendix of HR). Thus the long-time extreme excursions in the elastic system, which are not described by the effective potential, appear to stem from the finiteness of the piston mass.

By analogy, we anticipate that the macroscopic equations (3)–(5) should describe the final state for the inelastic piston in the $m_2 \to \infty$ limit. On the other hand, the log-periodic state emerges only when the piston mass is finite. This feature seems to play a parallel role as in the elastic system, in that departures from the predictions of the macroscopic equation arise only when the piston mass is finite.

IV. EFFECTIVE RESTITUTION COEFFICIENT

To understand the properties of the log-periodic oscillations, we map the three-particle system onto an equivalent two-particle system, from which the basic characteristics of the log-periodic state follow. The first step is to determine the net effect of the sequence of rattling collisions between the piston and a light particle as the piston approaches a wall and is ultimately reflected. We show in the Appendix that this collision sequence is equivalent to a one-body problem in which the piston is reflected from the wall with an effective restitution coefficient $r_{\rm eff}(m_2, r)$ that is smaller than the bare restitution coefficient r.

Next, we exploit the symmetry breaking, in which the piston localizes near one wall, to reduce the initial three-body problem into an effective two-body problem that con-

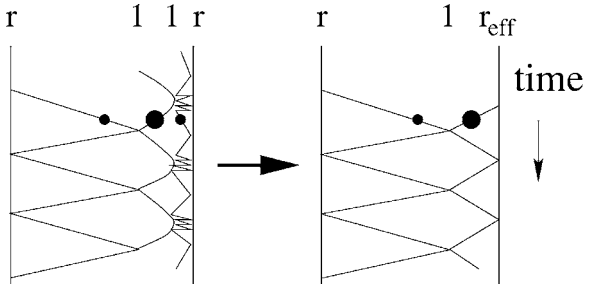

FIG. 6. Schematic space-time diagram of the particle trajectories in the log-periodic state (left) and the effective trajectories (right).

sists of the piston and one light particle. In this reduced system, the piston collides inelastically with the wall with restitution coefficient r_{eff}, while the light particle collides elastically with the piston and inelastically with the other wall with restitution coefficient r (Fig. 6). Using this equivalence, we will determine the properties of the log-periodic state.

For the initial step of determining the effective restitution coefficient as a function of r and m_2, the calculational details are given in the Appendix and the final result for $r_{\text{eff}}(m_2,r)$ is quoted in Eq. (A12). As shown in Fig. 7, r_{eff} decreases as r decreases and goes to zero as r approaches a critical value $r_c(m_2)$, quoted in Eq. (A7), that signals inelastic collapse. When $r<r_c$, the effective restitution coefficient is zero, and the result of the rattlings between the piston and the intervening light particle is inelastic collapse. For fixed r, notice also that r_{eff} decreases rapidly as m_2 is increased.

With this effective restitution coefficient equivalence, we now reduce the original three-particle system to the equivalent two-particle system. Without loss of generality, we assume that the piston is close to the wall at $x=1$. The effective system then consists of a light particle at x_1 and the piston at x_2, with $0<x_1<x_2<1$. For sufficiently large piston mass, the sequence of collisions consists of: (i) the piston making

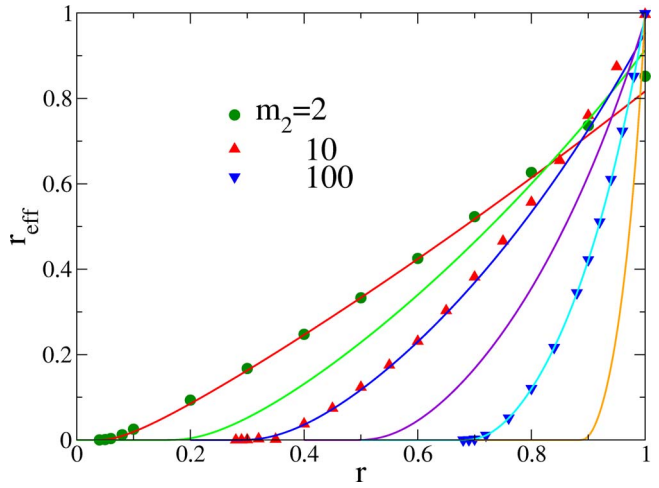

FIG. 7. (Color online) The effective restitution coefficient as a function of r for piston masses $m_2=2$, 5, 10, 30, 100, and 1000. The initial velocities are $(v_1,v_2)=(0,-1)$. The curves are the theoretical predictions from Eq. (A12), and the symbols correspond to simulation results.

an effective collision with the wall with restitution coefficient r_{eff}, (ii) the second light particle undergoing a bare inelastic collision with the other wall, and (iii) an elastic particle-piston collision, with each of these steps being nonoverlapping. From the collision rules for each of these steps [see Eqs. (A1) and (A2)], the new velocities after each such collision sequence are given in terms of the incoming velocities by

$$\begin{pmatrix} v_1' \\ v_2' \end{pmatrix} = \begin{pmatrix} \frac{m_2-1}{M} r & -\frac{2m_2}{M} r_{\text{eff}} \\ -\frac{2}{M} r & -\frac{m_2-1}{M} r_{\text{eff}} \end{pmatrix} \begin{pmatrix} v_1 \\ v_2 \end{pmatrix} \equiv \mathbf{L}\mathbf{v}, \quad (6)$$

where $M=1+m_2$, and $v_1,v_1'<0$ and $v_2,v_2'>0$. The velocity vector after n such cycles is $\mathbf{v}^{(n)}=\mathbf{L}^n\mathbf{v}$. Diagonalizing $\mathbf{L}$, we find (see the Appendix)

$$v_1^{(n)} = \frac{\Lambda_+^n(\Lambda_- - a) - \Lambda_-^n(\Lambda_+ - a)}{\Lambda_- - \Lambda_+} v_1 + \frac{b(\Lambda_-^n - \Lambda_+^n)}{\Lambda_- - \Lambda_+} v_2, \quad (7)$$

$$v_2^{(n)} = \frac{(\Lambda_+^n - \Lambda_-^n)(\Lambda_+ - a)(\Lambda_- - a)}{b(\Lambda_- - \Lambda_+)} v_1 + \frac{\Lambda_-^n(\Lambda_- - a) - \Lambda_+^n(\Lambda_+ - a)}{\Lambda_- - \Lambda_+} v_2, \quad (8)$$

where $a=r(m_2-1)/M$ and $b=-2r_{\text{eff}}m_2/M$ are the elements in the first row of $\mathbf{L}$, and $\Lambda_\pm$ are the eigenvalues of matrix $\mathbf{L}$,

$$\Lambda_\pm = \frac{m_2-1}{2M}(r-r_{\text{eff}})\left(1 \pm \sqrt{1+\frac{4rr_{\text{eff}}M^2}{(m_2-1)^2(r-r_{\text{eff}})^2}}\right). \quad (9)$$

Both eigenvalues are real, with $\Lambda_-<0$, $\Lambda_+>0$, and $|\Lambda_-|<|\Lambda_+|<1$.

We test this effective description of the collision dynamics by comparing the exact piston trajectory in the three-particle system for a given m_2 and r with the piston trajectory in the reduced two-particle system. After shifting the effective trajectory by an overall phase factor, both systems have visually indistinguishable periodic behavior, thus confirming the validity of the coarse-grained approach.

We now determine the relation that $v_1^{(n)}$ and $v_2^{(n)}$ must satisfy for the effective two-particle system to be in a log-periodic state. For such a periodicity, successive collisions between particle 1 and the piston must occur at the same position x_0 for all n. Thus the time $\delta t_i^{(n)}$ for particle i to go from x_0 to its respective wall and return to x_0 in the n^{th} cycle must be the same for both particles. That is,

$$\delta t_1^{(n)} = \frac{x_0}{|v_1^{(n)}|}\frac{1+r}{r} = \delta t_2^{(n)} = \frac{1-x_0}{|v_2^{(n)}|}\frac{1+r_{\text{eff}}}{r_{\text{eff}}} \equiv \delta t^{(n)}.$$

Thus

$$\frac{|v_2^{(n)}|}{|v_1^{(n)}|} = \frac{1-x_0}{x_0}\frac{r(1+r_{\rm eff})}{r_{\rm eff}(1+r)} \tag{10}$$

is a constant that is independent of n in the log-periodic state. Therefore $|v_2^{(n+1)}|/|v_1^{(n+1)}| = |v_2^{(n)}|/|v_1^{(n)}|$. Then using $\mathbf{v}^{(n+1)} = \mathbf{L}\mathbf{v}^{(n)}$, we express $\mathbf{v}^{(n+1)}$ in terms of $\mathbf{v}^{(n)}$ and thereby obtain

$$\frac{|v_2^{(n)}|}{|v_1^{(n)}|} = \frac{(1+m_2)\Lambda_+ - (m_2-1)r}{2m_2 r_{\rm eff}}, \tag{11}$$

where $\Lambda_+(m_2,r)$ is the larger eigenvalue of $\mathbf{L}$. Comparing Eqs. (10) and (11) finally yields

$$x_0 = \left(1 + \frac{(1+r)[(1+m_2)\Lambda_+ - (m_2-1)r]}{2m_2 r(1+r_{\rm eff})}\right)^{-1}, \tag{12}$$

and the amplitude of the piston oscillations is then $A(m_2,r) = 1-x_0$. This result agrees with the simulation results shown in Fig. 4, even close to inelastic collapse.

We may also compute the logarithmic period of the piston oscillations. Since $\delta t^{(n+1)}/\delta t^{(n)} = |v_2^{(n)}|/|v_2^{(n+1)}|$, we express $|v_2^{(n+1)}|$ in terms of $|v_1^{(n)}|$ and $|v_2^{(n)}|$ from Eq. (8), and then use Eq. (11) to obtain

$$\frac{\delta t^{(n+1)}}{\delta t^{(n)}} = \frac{\Lambda_+ - \dfrac{m_2-1}{1+m_2}r}{r_{\rm eff}\left(r - \dfrac{m_2-1}{1+m_2}\Lambda_+\right)} > 1. \tag{13}$$

Thus in the log-periodic state $\delta t^{(n)}$ grows exponentially in the number of cycles n, as seen in our simulations. From the logarithmic period $\Delta(m_2,r)$ introduced in Sec. II B, we have $t_{n-1} = e^{-\Delta} t_n$, so that $\delta t^{(n)} = t_n(1-e^{-\Delta})$. This relation then gives $\Delta = \ln(t_{n+1}/t_n) = \ln(\delta t^{(n+1)}/\delta t^{(n)})$. The agreement between this prediction for Δ with simulation results (not shown) is again extremely good.

Finally, the robustness of the log-periodic state can be understood in simple terms. Starting with an arbitrary (not log-periodic) initial state, it is easy to show from Eqs. (7) and (8) that both $v_1^{(n)}$ and $v_2^{(n)}$ converge exponentially quickly with n to a state where the ratio $|v_2^{(n)}|/|v_1^{(n)}|$ satisfies the condition (11) that signals log-periodicity. This convergence occurs because for $r_{\rm eff} < r$, $(\Lambda_-/\Lambda_+)^n$ quickly goes to zero as n increases. In this sense, the log-periodic state is an attractor of the dynamics.

V. SUMMARY

We investigated the dynamics of a three-particle system on the unit interval in which a massive particle (corresponding to a piston) lies between two light particles. The particles collide elastically with the piston, but inelastically with the walls. This toy model is meant to mimic the behavior of the inelastic piston problem in which a massive piston separates two inelastic gases, each of which contains many particles. The dynamics of this many-body problem is extremely rich. The piston moves nonmonotonically at early times and correspondingly the response of the two gases is also nonmonotonic. Eventually there is an inelastic collapse in which one of the gases is compressed into a solid by the piston.

One of the motivations for our study of the three-particle system was to capture some of the intriguing phenomenology of the many-particle inelastic piston problem. A new feature of the three-particle system, however, is that the piston settles into a log-periodic state at long times over a wide range of restitution coefficients, in which the period is constant on a logarithmic time scale. The characteristics of this log-periodic state can be understood in terms of a simple effective picture in which the rattling collision sequence between the piston and the trapped light particle is replaced by an effective inelastic collision between the piston and the wall, with effective restitution coefficient $r_{\rm eff} < r$. This equivalence provides a satisfyingly complete account of the log-periodic state. Finally, it should be noted that the log-periodic behavior is a consequence of the finiteness of the piston mass. As m_2 increases, the amplitude of the oscillations decreases and as $m_2 \to \infty$ the inelastic collapse of the many-particle inelastic piston problem is recovered.

ACKNOWLEDGMENTS

We thank R. Brito for collaboration during the initial stages of this project. S.R. thanks NSF Grant No. DMR0227670 (BU) and DOE Grant No. W-7405-ENG-36 (LANL) for financial support. P.I.H. acknowledges support from Spanish MEC, and thanks LANL and CNLS for hospitality during part of this project.

APPENDIX: CALCULATION OF THE EFFECTIVE RESTITUTION COEFFICIENT

We use a matrix approach to compute the effective restitution coefficient $r_{\rm eff}$ that describes the final velocity of the piston at the end of the rattling collisions as a function of m_2 and the bare restitution coefficient r. Without loss of generality, we assume that the piston compresses particle 1 which then undergoes the rattling collision sequence. For concreteness, the light particle is taken to be at rest at $x_1 > 0$ with a wall at $x=0$. A massive particle (the piston) approaches the light particle from the right with $v_2 = -1$. Collisions between particle 1 and the wall at $x=0$ are inelastic, with restitution coefficient r, while 1-2 collisions are elastic. After the rattling collision sequence ends, the piston recedes from the wall with velocity $v_2' = -v_2\, r_{\rm eff}$.

The velocities after each collision are given in terms of the velocities before the collision by

$$\begin{aligned} v_1' &= \frac{1-m_2}{M}v_1 + \frac{2m_2}{M}v_2, \\ v_2' &= \frac{2}{M}v_1 + \frac{m_2-1}{M}v_2, \end{aligned} \tag{A1}$$

for the 1–2 collision, and

$$\begin{aligned} v_1' &= -v_1\, r, \\ v_2' &= v_2, \end{aligned} \tag{A2}$$

for the wall collision, where $M = 1+m_2$. Thus the combined effect of a 1-2 and an ensuing particle-wall collision is given

by the composition of the two transformations implicit in Eqs. (A1) and (A2). Therefore

$$\begin{pmatrix} v_1' \\ v_2' \end{pmatrix} = \begin{pmatrix} -\frac{1-m_2}{M}r & -\frac{2m_2}{M}r \\ \frac{2}{M} & \frac{m_2-1}{M} \end{pmatrix} \begin{pmatrix} v_1 \\ v_2 \end{pmatrix} \equiv \mathbf{M}\mathbf{v}. \quad \text{(A3)}$$

The velocity vector after n such cycles is given by

$$\mathbf{v}^{(n)} = \mathbf{M}^n \mathbf{v}^{(0)}, \text{ with } \mathbf{v}^{(0)} = \begin{pmatrix} 0 \\ -1 \end{pmatrix}.$$

The collision sequence ends when the velocities of the two particles after n cycles satisfy $v_1^{(n)} - v_2^{(n)} < 0$, corresponding to the two particles receding from the wall with the piston moving faster than the light particle. We define this situation as "escape" of the piston. The number of collisions for escape to occur is given by the smallest value of n that leads to the above conditions on the outgoing velocities. The effective restitution coefficient is then given by $v_2^{(n)}$ when n equals its value at escape.

To determine the threshold value of n, we use the fact that (see, e.g., [16])

$$\mathbf{M}^n \mathbf{v} = \mathbf{S}\mathbf{M}_{\text{diag}}^n \mathbf{S}^{-1}\mathbf{v}, \quad \text{(A4)}$$

where $\mathbf{S}$ is the similarity matrix that diagonalizes $\mathbf{M}$, and $\mathbf{M}_{\text{diag}} = \mathbf{S}^{-1}\mathbf{M}^n\mathbf{S}$ is the diagonalized form of the transformation matrix. The eigenvalues of $\mathbf{M}$ are $\lambda_\pm = (T \pm \sqrt{T^2 - 4D})/2$, where $T = (m_2 - 1)(1+r)/M$ is the trace and $D = r$ is the determinant of $\mathbf{M}$,

$$\lambda_\pm = \frac{(m_2-1)(1+r)}{2M}\left(1 \pm \sqrt{1 - \frac{4rM^2}{(m_2-1)^2(1+r)^2}}\right). \quad \text{(A5)}$$

Consequently the similarity transformation matrix is

$$\mathbf{S} = \begin{pmatrix} 1 & 1 \\ \frac{\lambda_+ - a}{b} & \frac{\lambda_- - a}{b} \end{pmatrix},$$

where $a = r(m_2 - 1)/M$ and $b = -2m_2 r/M$ are the elements of the first row of $\mathbf{M}$, i.e., the matrix $\mathbf{S}$ consists of the eigenvectors of $\mathbf{M}$ arranged columnwise. Consequently $\mathbf{S}^{-1} = |\mathrm{S}|^{-1}\mathbf{S}^\dagger$, where $|\mathrm{S}|$ is the determinant of $\mathbf{S}$, and $\mathbf{S}^\dagger$ is its transpose.

Assembling these results, the velocity after n cycles (and $2n$ individual collisions) is

$$\mathbf{v}^{(n)} = \begin{pmatrix} b\frac{\lambda_+^n - \lambda_-^n}{\lambda_- - \lambda_+} \\ \frac{\lambda_+^n(\lambda_+ - a)}{\lambda_- - \lambda_+} - \frac{\lambda_-^n(\lambda_- - a)}{\lambda_- - \lambda_+} \end{pmatrix} \equiv \begin{pmatrix} v_1^{(n)} \\ v_2^{(n)} \end{pmatrix}. \quad \text{(A6)}$$

In the case where escape of the piston requires $n+1$ particle-particle collisions and n particle-wall collisions, we should multiply the transformation matrix $\mathbf{M}^n$ on the left by the matrix defined by Eq. (A1) to account for this last particle-particle collision. However, to compute only the final velocity of particle 2, it suffices to calculate $\mathbf{v}^{(n+1)}$ from Eq. (A6).

Depending on the sign of the discriminant $T^2 - 4D$, the eigenvalues $\lambda_\pm$ can be real or complex. For r greater than a threshold value $r_c(m_2)$, $T^2 < 4D$. Thus $\lambda_\pm$ are complex conjugates (note, however, that $\mathbf{v}^{(n)}$ has always real components). At the threshold, $T^2 = 4D$, leading to $\lambda_+ = \lambda_-$, so that $\mathbf{v}^{(n)}$ is undetermined. This indeterminacy signals inelastic collapse: for $r < r_c(m_2)$ there is an infinite number of collisions in a finite time, and $v_1^{(n)} - v_2^{(n)} > 0 \ \forall \ n$. The condition $T^2 = 4D$ gives the critical restitution coefficient for inelastic collapse:

$$r_c(m_2) = \frac{(1+m_2)(1+m_2-4\sqrt{m_2}) + 4m_2}{(m_2-1)^2}. \quad \text{(A7)}$$

Notice that $r_c \sim 1 - 4/\sqrt{m_2}$ in the limit of large m_2. Equivalently, the condition $T^2 = 4D$ defines a critical mass $\mu_c(r)$, such that inelastic collapse occurs for $m_2 > \mu_c(r)$. We now find

$$\mu_c(r) = \frac{(1+r)(1+r+4\sqrt{r}) + 4r}{(1-r)^2}. \quad \text{(A8)}$$

Note that for r close to 1, $\mu_c(r) \sim 16(1-r)^{-2}$.

For $r > r_c(m_2)$ the piston eventually escapes with velocity $v_2^{(n_0)}$, where n_0 is the number of cycles until escape. To determine n_0, define $f(n) \equiv v_1^{(n)} - v_2^{(n)}$. Initially $f(0) = 1$, and $f(n)$ decreases as n increases and eventually changes sign. Next, we define the real variable z by the condition $f(z) = 0$. From Eq. (A6),

$$f(z) = \frac{b(\lambda_+^z - \lambda_-^z) - \lambda_+^z(\lambda_+ - a) + \lambda_-^z(\lambda_- - a)}{\lambda_- - \lambda_+} = 0. \quad \text{(A9)}$$

Since $\lambda_\pm$ are complex conjugates, we write $\lambda_\pm = Q\, e^{\pm i\beta}$ so that Eq. (A9) becomes, using $\lambda_+^z - \lambda_-^z = 2iQ^z \sin(z\beta)$ and $a + b = -r$,

$$r \sin(z\beta) + Q \sin[(z+1)\beta] = 0, \quad \text{(A10)}$$

with solutions

$$z(k) = \frac{1}{\beta}\left[k\pi - \tan^{-1}\left(\frac{Q\sin\beta}{r + Q\cos\beta}\right)\right], \quad \text{(A11)}$$

where k can be any integer number. The first solution that has a physical meaning (i.e., $z > 1$) corresponds to $k = 1$, so $z = z(1)$. The number of collision cycles before escape is thus $n_0 = \lceil z \rceil$, where $\lceil z \rceil$ is the next integer larger than z. The escape velocity is $v_2^{(n_0)}$ and $r_{\text{eff}} = v_2^{(n_0)}$. However, for large enough piston mass, the number of collisions before escape is typically large, and we can approximate n_0 by z. Hence, we finally obtain for the effective restitution coefficient,

$$r_{\text{eff}}(m_2, r) = \frac{\lambda_+^z(\lambda_+ - a) - \lambda_-^z(\lambda_- - a)}{\lambda_- - \lambda_+}, \quad \text{(A12)}$$

with z given by Eq. (A11) with $k = 1$. A plot of r_{eff} as a function of r is given in Fig. 7.

[1] P. I. Hurtado and S. Redner, preceding paper, Phys. Rev. E **73**, 016136 (2006).
[2] H. B. Callen, *Thermodynamics* (J. S. Wiley & Sons, New York, 1960).
[3] E. H. Lieb, Physica A **263**, 491 (1999).
[4] E. Kestemont, C. Van den Broeck, and M. Malek Mansour, Europhys. Lett. **49**, 143 (2000).
[5] C. Gruber, S. Pache, and A. Lesne, J. Stat. Phys. **108**, 669 (2002).
[6] N. I. Chernov, J. L. Lebowitz, and Ya. G. Sinai, Russ. Math. Surveys **57**, 1045 (2002).
[7] G. Galperin and A. Zemlyakov, *Mathematical Billiards* (Nauka, Moscow, 1990) (in Russian).
[8] V. V. Kozlov and D. V. Treshshëv, *Billiards: A Generic Introduction to the Dynamics of Systems with Impacts* (American Mathematical Society, Providence, RI, 1991).
[9] S. Tabachnikov, *Billiards* (Société Mathématique de France American Mathematical Society, Providence, RI, 1995).
[10] E. Gutkin, J. Stat. Phys. **81**, 7 (1996).
[11] S. Redner, Am. J. Phys. **72**, 1492 (2004).
[12] R. Brito, M. J. Renne, and C. Van den Broeck, Europhys. Lett. **70**, 29 (2005).
[13] See, e.g., S. McNamara and W. R. Young, Phys. Fluids A **4**, 496 (1992); Phys. Rev. E **53**, 5089 (1996); I. Goldhirsch and G. Zanetti, Phys. Rev. Lett. **70**, 1619 (1993); P. Deltour and J.-L. Barrat, J. Phys. I **7**, 131 (1997).
[14] P. Haff, J. Fluid Mech. **134**, 401 (1983).
[15] Ya. G. Sinai, Theor. Math. Phys. **121**, 1351 (1999).
[16] See, e.g., G. Arfken and H. J. Weber, *Mathematical Methods for Physicists*, 5th ed. (Academic Press, New York, 2000).